

Mechanical and tribological properties of TiB₂-Ti composites prepared by spark plasma sintering

V. Puchý^{1*}, J. Kováčik², A. Kovalčíková¹, R. Sedlák¹, R. Džunda¹, J. Dusza¹, L. Falat¹, M. Podobová¹, M. Besterci¹, P. Hvizdoš¹

¹*Institute of Materials Research, Slovak Academy of Sciences, Watsonova 47, 040 01 Košice, Slovak Republic*

²*Institute of Materials and Machine Mechanics, Slovak Academy of Sciences, Dúbravská cesta 9/6319, 845 13 Bratislava, Slovak Republic*

Received 17 June 2019, received in revised form 5 August 2019, accepted 7 August 2019

Abstract

The TiB₂-Ti composites with different concentrations of the Ti metallic second phase were prepared by the spark plasma sintering. We investigated the tribological properties of TiB₂ and TiB₂-Ti materials by ball-on-disc technique on the HTT CSM tribometer under loads of 1, 5, and 10 N. The wear tracks morphology was investigated by scanning electron and confocal microscopy. The microstructures of the TiB₂ + Ti materials consist of a small-grained matrix with relatively well dispersed TiB₂ particulate grains. The wear test results show that the wear rate of composites is gradually reduced over the sliding speed range for all normal loads. The composite wear rates are lower than the monolith ones. The Ti phase played a dual role in improving the tribological properties of the TiB₂-Ti composites by acting as a lubricant and in increasing the fracture toughness by influencing the microstructure and mechanical properties.

Key words: TiB₂-Ti composites, spark plasma sintering, coefficient of friction, wear

1. Introduction

The titanium diboride ceramic is very hard, electrically and thermally conductive, wear, and high-temperature resistant material with high elastic modulus. All these properties are beneficial for many applications like cutting tools, armors, turbine blades, and wear-resistant parts working in severe conditions. However, the fabrication of pure titanium diborides is a challenging task, and obtaining a sufficient density requires high sintering temperature and long dwell time. Such conditions lead to significant grain growth, which causes a drop in mechanical properties, mainly fracture toughness and flexural strength [1–3]. This unfavorable fact leads to the increasing effort of the scientific community in the investigation of composites based on titanium diboride. With the addition of metallic binders, the fracture toughness of TiB₂-based materials increased from 3–5 to 6–12 MPa m^{1/2} due to the plastic deformation of the metallic phase and crack bridging toughening [4–6]. The TiB₂-Ti materials are

interesting, thanks to their excellent mechanical and electrical properties. The present paper deals with the influence of the two different sintering temperatures and two different sintering pressures on the density and microstructure of TiB₂ and TiB₂-Ti materials. In the present study, TiB₂ and TiB₂-Ti composites were made by a method called pulsed electric current sintering (PECS) or spark plasma sintering (SPS). This sintering technique has the advantage of higher heating rates and shorter dwell times in comparison with conventional methods [7, 8]. It is considered that the SPS prepared TiB₂ material will be used for the surface treatment of titanium and titanium alloys via electro spark deposition (ESD) method [9]. ESD deposition enables to product hard and wear-resistant coatings on metallic substrates. The only essential condition is that both substrate and electrode materials ought to be electrically conductive. A significant advantage is that due to the diffusion of electrode material into the substrate and vice versa relatively good bonding between the layer and the substrate occurs. ESD method

*Corresponding author: e-mail address: vpuchy@saske.sk

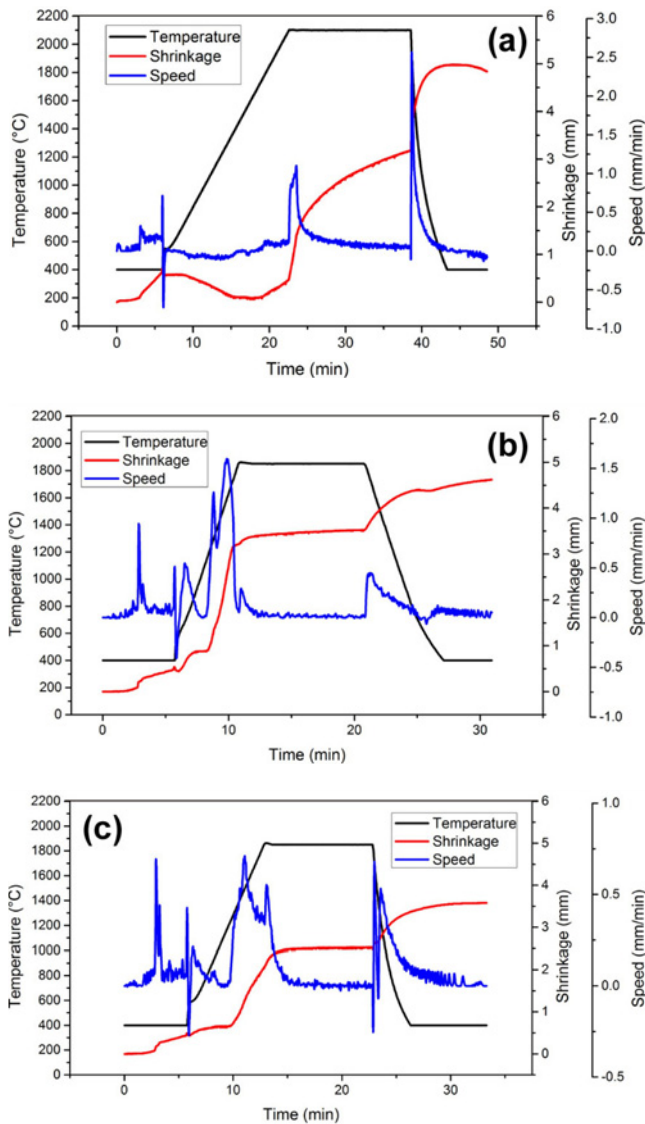


Fig. 1. Temperature and shrinkage cycles during SPS process of TiB₂ (a), TiB₂-15%Ti (b), and TiB₂-20%Ti (c).

enables to use titanium and titanium alloys (thanks to increase of their surface hardness and wear resistance) as sonotrode cutting tools [10] and also for biomedical applications in tooth impacts [11]. In this paper, the wear properties of TiB₂ and TiB₂-Ti composites with 15 and 20 % Ti, under various applied loads are presented. Excellent low wear rate has been achieved, and the wear mechanisms have been discussed.

2. Experimental materials and methods

2.1. Materials preparation and characterization

TiB₂ powder of angular shape (purity 99 %, -400

mesh, supplied by ESK Ceramics GmbH & Co. KG, Germany) was used as a matrix powder for the investigations. Further, Ti powder (purity 99.4 %, supplied by Kimet Special Metal Precision Casting Co., Ltd., China) is also of typical angular shape due to the HDH preparation method. The powder size distributions were determined using Fritch Analysette 22 laboratory equipment. For Ti powder it is $d_{10} = 12 \mu\text{m}$, $d_{50} = 25 \mu\text{m}$, and $d_{90} = 45 \mu\text{m}$. In the case of TiB₂ it is $d_{10} = 4 \mu\text{m}$, $d_{50} = 16 \mu\text{m}$, and $d_{90} = 34 \mu\text{m}$. The TiB₂ with Ti powder mixture was dry-mixed in Turbula mixer (WAB AG, Switzerland) for 30 min prior to the SPS. The TiB₂-Ti powder was loaded into a graphite die with an inside diameter of 20 mm. SPS (Type HP D 10SD, FCT Systeme, Germany) was performed in a vacuum (5 Pa). A pulsed direct electric current was applied with a pulse duration of 15 ms and pause time of 3 ms throughout all the experiments. The temperature was measured using a top pyrometer focused inside a hole in the punch at a distance of 4 mm from the sample. In the present study, the SPS schedule was varied to assess the effects of temperature, heat rate, and pressure on the samples, as shown in Fig. 1. In all experiments, a minimum pressure of 7 MPa was applied to ensure constant contact of the electrodes with the die/punch/sample system. The die/punch assembly was wrapped in a graphite insulating felt and placed inside the SPS. The powder was then heated in low vacuum (10 Pa). The monolithic TiB₂ was densified at 2100 °C and 50 MPa for 15 min, while composites were densified at 1850 °C and 35 MPa for 10 min. The sintering temperature for the composites was selected based on the fact that the melting point of Ti is 1668 °C. The density was found using the Archimedes method, hardness and indentation fracture toughness by indentation methods using Vickers diamond tip loaded by 9.81 N. After SPS sintering and grinding, the sintered discs had a thickness of 4 mm and diameter of 20 mm. The samples were subsequently polished with a diamond suspension to a 1 μm finish. The apparent density of the sintered composites was measured in ethanol by the Archimedes method. The microstructure of the sintered composites were examined by scanning electron microscopy (SEM, Jeol JSM-7000F, Netherlands), equipped with an energy dispersive spectrometer analysis system (EDS) for compositional analysis. The average TiB₂-Ti and TiB₂ grain size was determined from SEM micrographs using *Image-J* software for Windows. The friction and wear behavior of monolithic TiB₂ and TiB₂-Ti composite disks were studied using a tribometer HTT by CSM Instruments in air at the room temperature using the ball-on-disc technique, where the tribological partner for each material was a polished ball with 6 mm diameter made out of SiC corresponding to the ceramic matrix of the tested material. The applied load was 1, 5, and 10 N, the sliding speed 0.1 ms⁻¹, and the

Table 1. Microstructure parameters and mechanical properties of the investigated materials

Experimental materials	Apparent density (g cm ⁻³)	Relative density (%)	Hardness HV1 (GPa)	Fracture toughness (MPa m ^{1/2})
TiB ₂	4.378	96.9	19.42 ± 4.85	5.86 ± 0.36
TiB ₂ + 15%Ti	4.153	91.9	8.83 ± 1.41	5.92 ± 0.41
TiB ₂ + 20%Ti	4.452	98.5	12.54 ± 2.63	8.35 ± 0.65

Table 2. Tribological and wear properties of investigated materials

Experimental materials	Applied load (N)	Distance (m)	COF (-)	Wear rate × 10 ⁻⁶ (mm ³ m ⁻¹ N ⁻¹)
TiB ₂	1	500	0.542 ± 0.086	6.05 ± 0.30
	5	500	0.658 ± 0.054	4.51 ± 0.23
	10	500	0.554 ± 0.046	16.98 ± 1.19
TiB ₂ + 15%Ti	1	500	0.393 ± 0.077	1.98 ± 0.11
	5	500	0.634 ± 0.033	1.60 ± 0.08
	10	500	0.661 ± 0.048	2.16 ± 0.12
TiB ₂ + 20%Ti	1	500	0.861 ± 0.118	1.93 ± 0.12
	5	500	0.531 ± 0.019	0.77 ± 0.05
	10	500	0.313 ± 0.029	0.66 ± 0.04

sliding distance was 500 m. The worn surfaces were subsequently observed and the wear regimes, damage type, and micromechanisms were identified. The tests were conducted according to the ASTM G99-95a standard.

3. Results and discussion

3.1. Sintering behavior

The relative density of the TiB₂ and TiB₂-Ti composites, spark plasma sintered according to the two different loading cycles, is presented in Table 1. Relative densities below 98.5% were obtained in case of the composites sintered according to 35 MPa pressure cycle (Figs. 1b,c) and about 97% in case of the monolithic sample according to 50 MPa pressure cycle (Fig. 1a), respectively (Table 1). Due to the residual porosity, the TiB₂-Ti composites with lower Ti volume exhibited a much lower density than the corresponding monolithic samples. The difference in density and hardness, which is related to a different densification behavior, clearly demonstrates that the pressure cycle applied during pulsed electric current sintering strongly influences the sintering behavior of the TiB₂

and TiB₂-Ti composites and also their microstructural and physical properties. The densification behavior during sintering, i.e., the shrinkage and shrinkage rate of the powder compacts were recorded, as shown in Fig. 1 for the TiB₂ and TiB₂-Ti composites processed using the two different loading cycles. The densification curves of the monolithic and composite samples show a different densification behavior as can be seen from Fig. 1. In the case of the monolithic sample, the densification process starts at 2100°C, while in the case of a composite sample, this process starts already at approx. 1495°C, which is 605°C lower temperature than for the monolithic sample. The axial dimension shrinkage firstly decreases and then increases. This may be due to the thermal expansion during the heating stage, similarly as it was reported for Ti₃SiC₂/Pb composites [12]. As the temperature gradually increased, the diffusion rate of atoms increased, which manifests as a decreasing trend in the axial dimension. At approx. 1592°C maximum piston travel speed in the case of composites was reached, where the liquid Ti phase contributed to maximum densification speed. The maximum density (~ zero piston travel speed) was reached at 5 min after started dwell time in the monolithic material and at approx. 2 min in the composite materials.

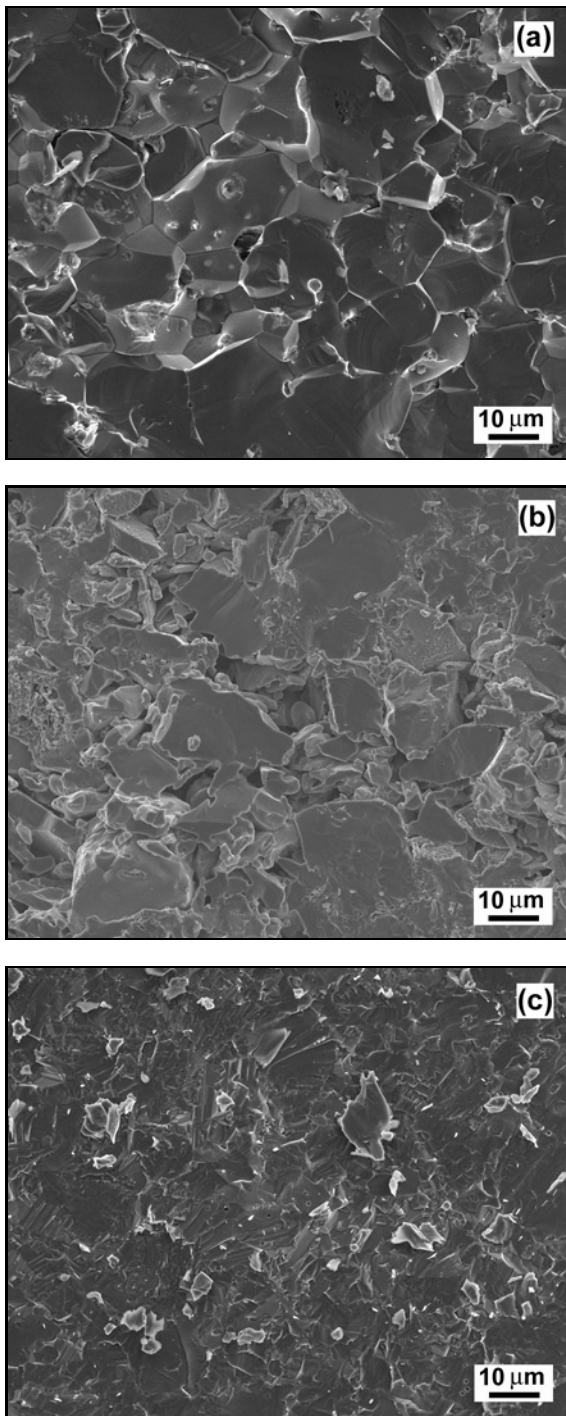


Fig. 2. SEM images of the fracture surface of TiB₂ (a), TiB₂-15%Ti (b), and TiB₂-20%Ti (c).

3.2. Microstructure and mechanical properties

The study was performed to identify significance and influence of process parameters on microstructure, coefficient of friction, and wear of spark plasma sintered TiB₂-Ti composites. Measured results of microstructures, mechanical properties, and tribological

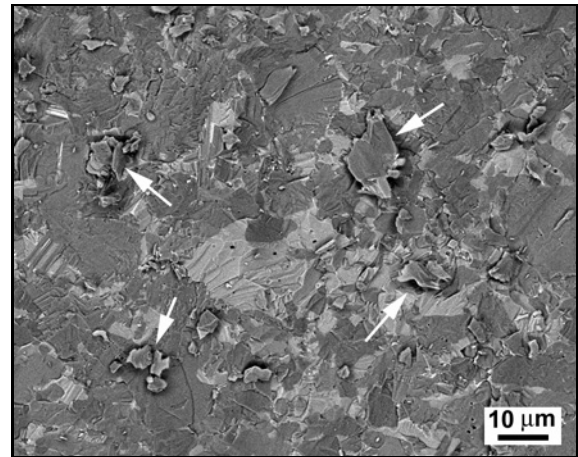


Fig. 3. SEM micrograph of the composite fracture surface. Arrows indicate the plastic deformation of the Ti metallic phase.

parameters are summarized in Tables 1 and 2. Monolithic TiB₂ samples sintered at temperature 2100 °C with a holding time of 10 min attained 96.9 % of theoretical density whereas TiB₂-Ti samples sintered at the relatively low temperature 1850 °C attained from 91.9 to 98.5 %. Figure 2 shows the fracture surface of the sintered samples. In monolithic TiB₂ (Fig. 2a), microstructure exhibits no grain growth, contains some porosity (< 3 %), and the average grain size is 25 μm. Figure 2b shows the least dense microstructure of TiB₂ containing 15 % Ti. The Ti phase is interconnected and relatively homogeneously distributed in the TiB₂ matrix (Figs. 2b,c). With further increasing amount of Ti, the composite density increases (Table 1). Vickers hardness tests specify that the composite materials have a much lower hardness. The comparative indents of those four materials were made with 9.81 N load. The hardness of monolith material is about 19.4 GPa while that of the composite materials is much lower and reaches a maximum of about 12.5 GPa for TiB₂-20%Ti.

3.3. Friction and wear

Table 2 shows the volumetric wear rates of TiB₂ and TiB₂-Ti at different sliding speeds and loads. Figure 4 shows the worn surface of the monolith and composite specimens under 10 N force. Numerous surface changes in the form of scales, grooves, and scratch marks are evident on the worn surface, which are the characteristics of abrasion and adhesion. Figure 4a is the worn surface of the monolith; scales and grooves are evident on the worn surface. Figure 4b is the worn surface of the composite, compared with the matrix it has flatter grooves and less scaly marks. This is mainly because the toughness and density of the composites are higher than those of the monolith ceramic.

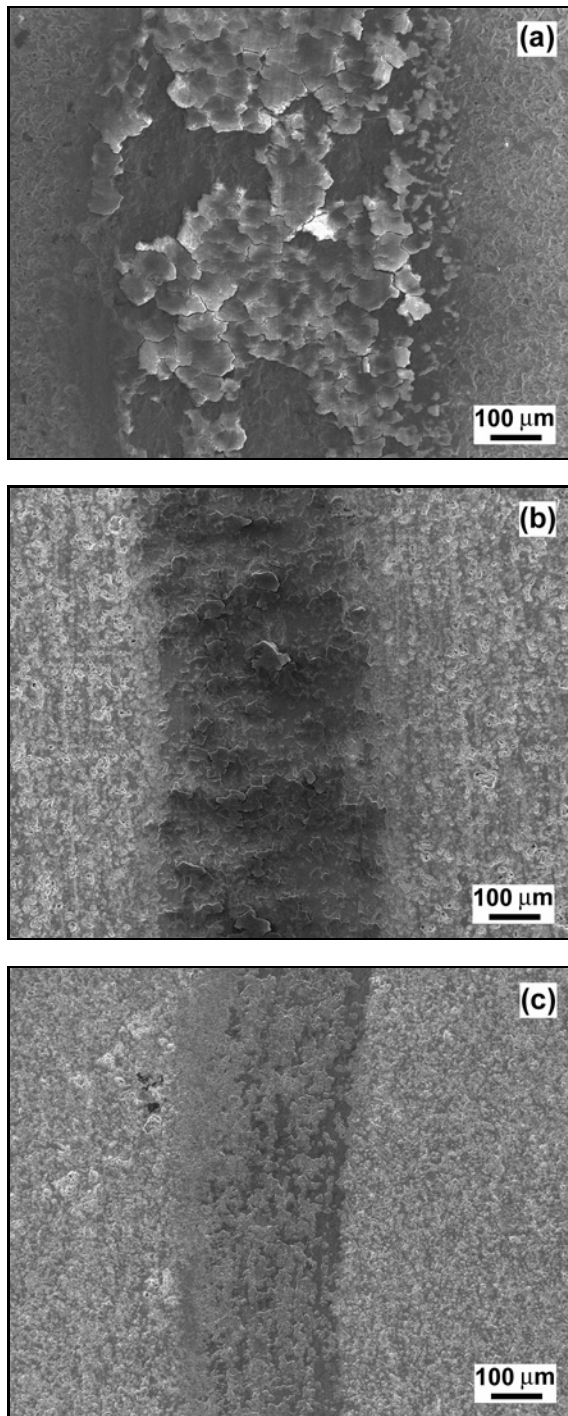


Fig. 4. Surface morphology after adhesion – wear track of TiB_2 (a), TiB_2 -15%Ti (b), and TiB_2 -20%Ti composite (c) by force 10 N and rotation speed 0.1 m s^{-1} .

Abrasion is caused by hard roughness on the SiC counterface (Fig. 5) or hard particles released/pulled out from material in between the contacting surfaces, which can be a result of plowing or cutting but mostly a combination of both. While cutting creates cut marks in the worn surface, the released debris is in

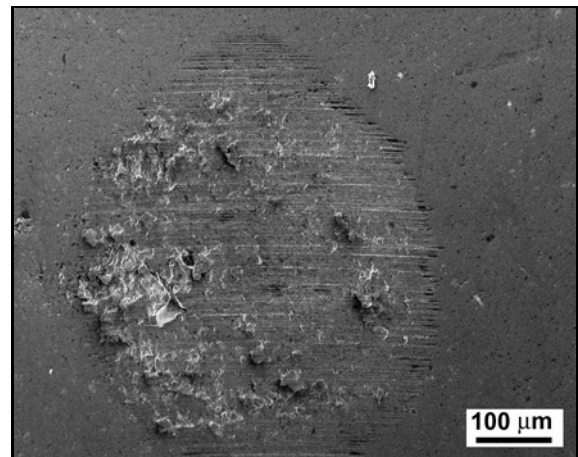


Fig. 5. Worn surface morphology of the counterpart SiC ball surface.

the form of scales or ribbons, similar to the results observed by other authors [13, 14].

We analyzed debris of the composites and matrix under the 10 N load by SEM with EDX and found that the wear debris was scales and flakes or debris layers, as shown in Figs. 6–8. However, the occurrence of such types in the wear debris is rare. This suggests that abrasion takes place primarily via plowing. Studying the reasons for grooving and scratching, there are the following two reasons. The ball SiC counterface creates hard debris on the surface while rubbing against the sample; because the hardness of the samples is lower than that of the SiC ball, debris of the ceramic composite would plow or engrave into the surface of samples. As wear progresses under the low load, the worn surface creates powdery debris due to oxidation, some of this debris exists in the contacting surfaces of the SiC ball and samples, this powdery debris plows or engraves into the surface of samples during the wear, so the surface of the samples shows grooves and scratch marks. The wear mechanism of the composites and matrix oxidative changes with the load increase.

For the monolithic TiB_2 material, when the load was 5 N, the worn surface appeared darker, the wear debris was the powder black SiC (Figs. 6, 7), and the wear mass loss decreased. This means that the matrix caused oxidative wear. When the load was 10 N, visual inspection revealed that the metallic fragments existed in the SiC counterface; these fragments were gradually pulled out and became the wear debris in the form of scales, Fig. 9a, and they were confirmed with EDS analysis, Fig. 9b.

For the composites, the worn surface color became dark, and the wear mass loss decreased when the load was 10 N. This means that the composites suffered oxidative wear under this load. Compared with the monolithic matrix, the color of the worn composite surfaces under the load of 10 N was darker than that

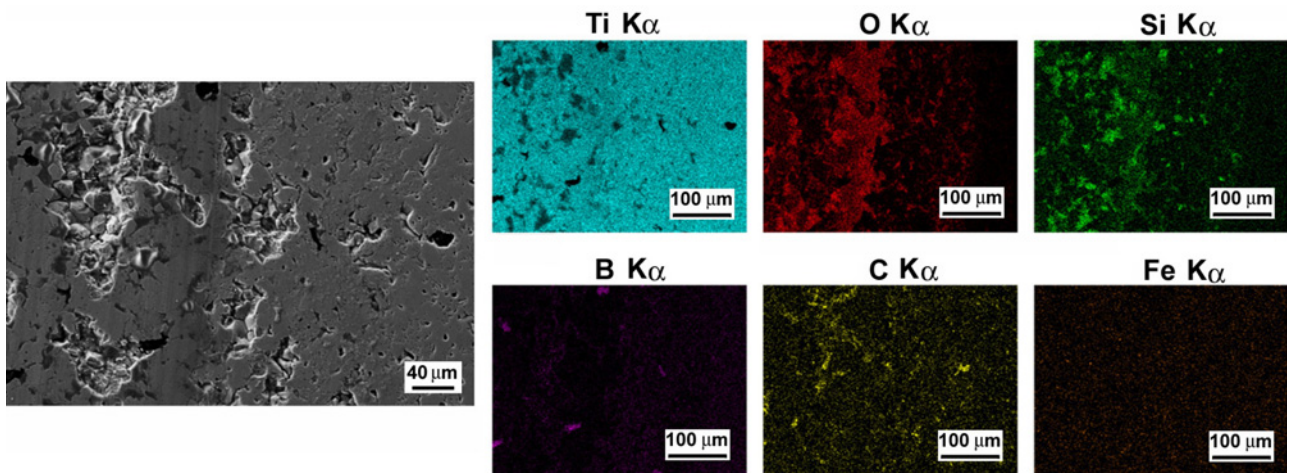


Fig. 6. Surface morphology of the monolith after adhesive wear (left portion) with EDX images (right portion) of TiB_2 wear track.

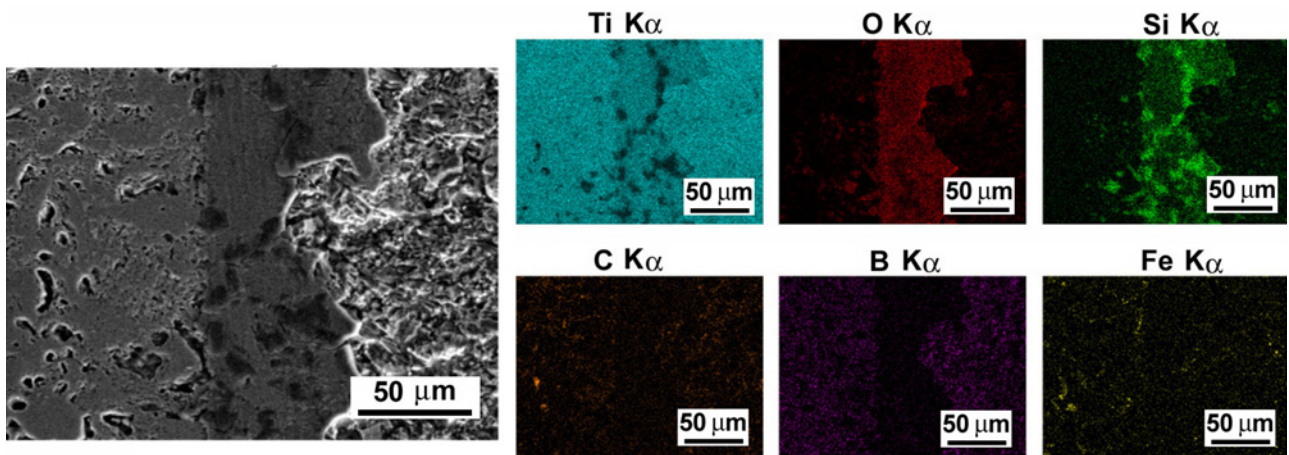


Fig. 7. Surface morphology of the composite after adhesive wear (left portion) with EDX images (right portion) of TiB_2 -15%Ti wear track.

of the monolithic matrix under the load of 5 N, and the wear mass loss was less than that of the monolithic matrix. This indicates that the oxide film of the composites is more durable than that of the monolithic matrix, and it can better prevent the surface of the composites from directly contacting with the SiC counterface, which leads to the wear mass loss of the composites less than that of the monolithic matrix.

The friction tracks made on samples using 10 N load were observed by confocal microscopy (Fig. 9). The width and depth of the friction tracks are bigger in the monolithic material and decreasing with increasing in ductile Ti content in the composites, which could reflect the increase in fracture toughness and also increasing trend in hardness (Table 1).

4. Summary

The wear behavior of TiB_2 -Ti composites with a

various volume of Ti was studied using a ball-on-disc method. These materials were prepared by spark plasma sintering. The increase in Ti content improves the wear resistance of the composites. The normal force load has a significant effect on the tribological properties of the composites. The friction coefficient is affected by the load values. The application of higher load firstly decreases the friction coefficient of the composite with the content of 20 vol.% Ti, but with 15 vol.% Ti COF again slightly increased. The reduction of wear rate with increasing the volume Ti and size of the normal load was observed. The best value of friction coefficient (0.31) and specific wear rate ($0.66 \times 10^{-6} \text{ mm}^3 \text{ N}^{-1} \text{ m}^{-1}$) have the composites with 20 vol.% Ti which were obtained at the temperature of 1850 °C and 35 MPa for 10 min. The sintering processing conditions were optimized to obtain homogeneously dispersed and dense TiB_2 -Ti composites by SPS. In composite with 20 vol.% Ti, an effective toughening was achieved in such a way that its tough-

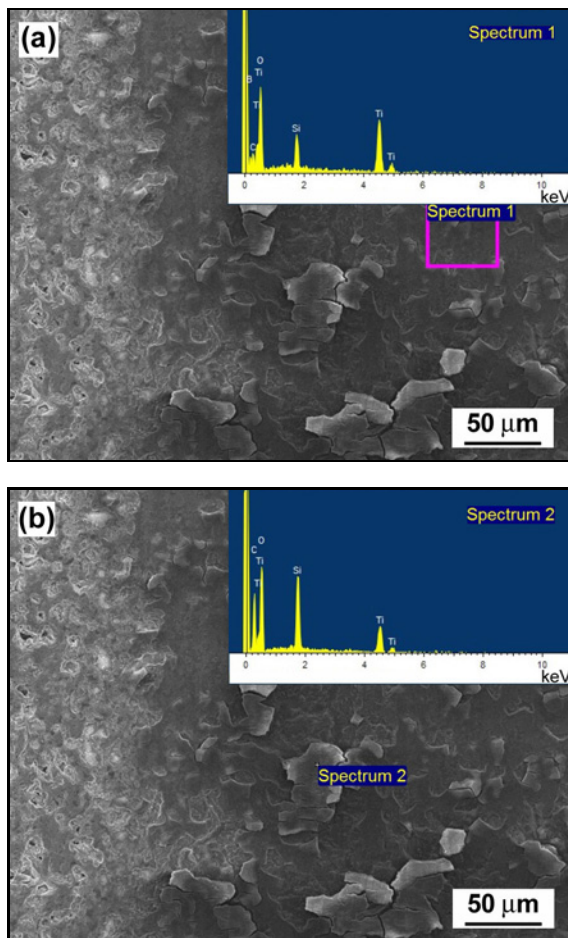


Fig. 8. Surface morphology detail of the composite after adhesive wear, wear track for TiB_2 -15%Ti composite with EDS, square area is from wear track (a), the local spectrum from scurf (b), by force 10 N and rotation speed 0.1 m s^{-1} .

ness was approximately 1.4 times higher than that of both 15 vol.% Ti composite and monolithic TiB_2 . The wear loss in the composites is much less sensitive to increase of the normal load than in monolithic TiB_2 .

Acknowledgements

This work was supported by the Slovak Research and Development Agency under the contract No. APVV-15-0469 and was also realized within the frame of the project Research Centre of Advanced Materials and Technologies for Recent and Future Applications “PROMATECH”, which is supported by the Operational Program “Research and Development” financed through European Regional Development Fund.

References

- [1] Chao, S., Goldsmith, J., Banerjee, D.: *Int J Refract Met H*, 49, 2015, p. 314.
[doi:10.1016/j.ijrmhm.2014.06.008](https://doi.org/10.1016/j.ijrmhm.2014.06.008)

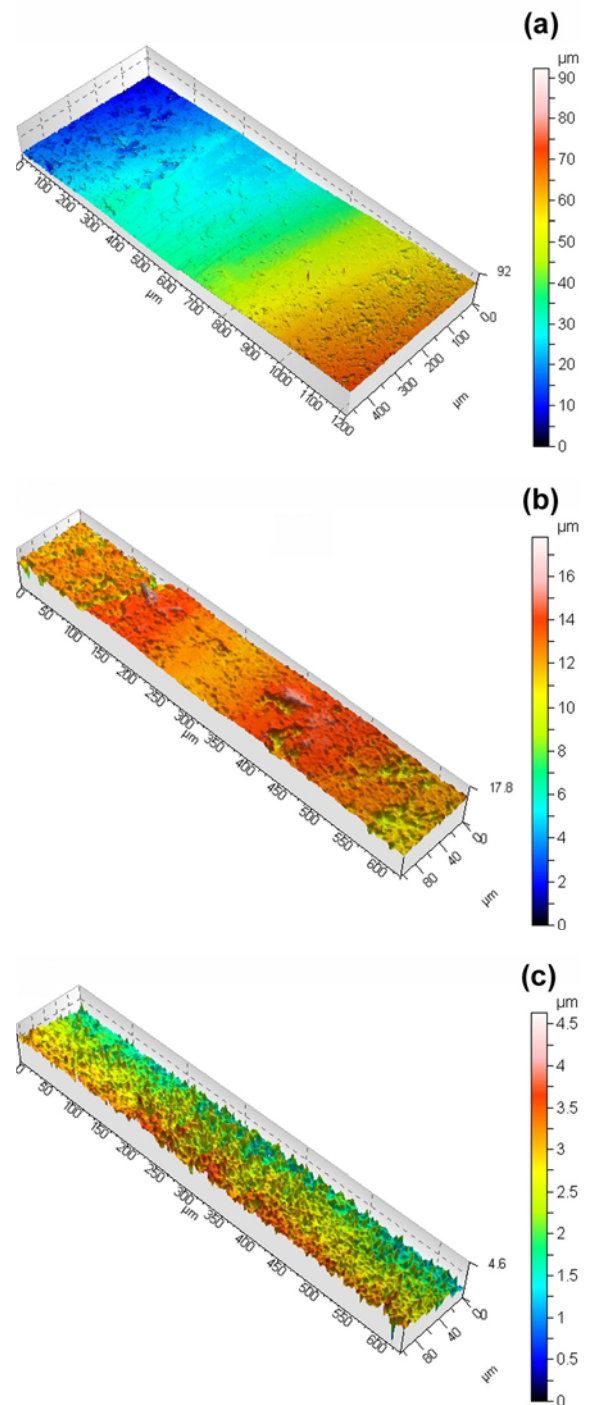


Fig. 9. Axonometric plots of monolith TiB_2 (a), TiB_2 -15%Ti (b), and TiB_2 -20%Ti (c) friction track surface, by force 10 N and rotation speed 0.1 m s^{-1} , showing decreasing wear with increasing Ti content.

- [2] Wang, W., Fu, Z., Wang, H., Yuan, R.: *J Eur Ceram Soc*, 22, 2002, p. 1045.
[doi:10.1016/S0955-2219\(01\)00424-1](https://doi.org/10.1016/S0955-2219(01)00424-1)
- [3] Li, B.: *Int J Refract Met H*, 46, 2014, p. 84.
[doi:10.1016/j.ijrmhm.2014.05.019](https://doi.org/10.1016/j.ijrmhm.2014.05.019)

- [4] Chlup, Z., Bača, L., Halasová, M., Neubauer, E., Hadraba, H., Stelzer, N., Roupcová, P.: *J Eur Ceram Soc*, 35, 2015, p. 2745. [doi:10.1016/j.jeurceramsoc.2015.03.027](https://doi.org/10.1016/j.jeurceramsoc.2015.03.027)
- [5] Fu, Z., Koc, R.: *J Am Ceram Soc*, 2017, p. 1. [doi:10.1111/jace.14814](https://doi.org/10.1111/jace.14814)
- [6] Sánchez, J. M., Azcona, I., Castro, F.: *J Mater Sci*, 35, 2000, p. 9. [doi:10.1023/A:1004763709854](https://doi.org/10.1023/A:1004763709854)
- [7] Orru, R., Licheri, R., Locci, A. M., Cincotti, A., Cao, G.: *Mater Sci Eng R Reports*, 63, 2009, p. 127. [doi:10.1016/j.mser.2008.09.003](https://doi.org/10.1016/j.mser.2008.09.003)
- [8] Omori, M.: *Mater Sci Eng A*, 287, 2000, p. 183. [doi:10.1016/S0921-5093\(00\)00773-5](https://doi.org/10.1016/S0921-5093(00)00773-5)
- [9] Emmer, Š., Baksa, P., Kováčik, J.: *Kovove Mater*, 53, 2015, p. 423. [doi:10.4149/km_2015_6_423](https://doi.org/10.4149/km_2015_6_423)
- [10] Kováčik, J., Baksa, P., Emmer, Š.: *Acta Metallurgica Slovaca*, 22, 2016, p. 52. [doi:10.12776/ams.v22i1.628](https://doi.org/10.12776/ams.v22i1.628)
- [11] Viskić, J., Schauerperl, Z., Čatić, A., Balog, M., Krizik, P., Gržeta, B., Popović, J., Ortolan, S. M., Mehulić, K.: *Acta Stomatologica Croatica*, 48, 2014, p. 285. [doi:10.15644/asc48/4/6](https://doi.org/10.15644/asc48/4/6)
- [12] Zhang, R., Feng, K., Meng, J., Su, B., Ren, S., Hai, W.: *Ceram Int*, 41, 2015, p. 10380. [doi:10.1016/j.ceramint.2015.05.013](https://doi.org/10.1016/j.ceramint.2015.05.013)
- [13] Bača, L., Lenčes, Z., Jogl, Ch., Neubauer, E., Vitkovič, M., Merstallinger, A., Šajgalik, P.: *J Eur Ceram Soc*, 32, 2012, p. 1941. [doi:10.1016/j.jeurceramsoc.2011.10.039](https://doi.org/10.1016/j.jeurceramsoc.2011.10.039)
- [14] Rabinowicz, E.: *Friction and Wear of Materials*. 2nd Edition. New York, Wiley-Interscience 1995. ISBN: 978-0-471-83084-9.